[Article ID] 1003- 6326(2001) 04- 0567- 05

Preparation and characterization of LPPS NiCoCrAlYTa coatings for gas turbine engine[®]

HONG Ruirjiang(洪瑞江), ZHOU Kersong(周克崧), WANG Derzheng(王德政), ZHU Huirzhao(朱晖朝), KUANG Zirqi(邝子奇) (Guangzhou Research Institute of Non-ferrous Metals, Guangzhou 510651, P. R. China)

[Abstract] NiCoCrAlYTa coatings have been deposited onto an aircraft gas turbine engine blade using a LPPS unit equipped with a computerized robot. Optimal processing conditions, including spray parameters, the trajectory of the robot, and the synchronized movements between the torch and the blade, have been developed for superior coating properties. Transferred arc treatment, providing a preheating and a cleaning of the substrate surface, enhances the adherence of the coatings to the substrate. The resulting LPPS coatings show dense and uniform characteristics with ideal hardness, and good corrosion resistance to cycle oxidation.

[**Key words**] low pressure plasma spraying; hot corrosion; coating; gas turbine engine; MCrAlY [**CLC number**] TG 174. 442 [**Document code**] **A**

1 INTRODUCTION

New high strength superalloys have been widely used in aircraft and power station gas turbine for their reliable operations under the conditions of high temperatures and high rotational speeds^[1,2]. In order to further improve their performances in resisting high temperature oxidation, hot corrosion, erosion and thermal fatigue, surface treatment is necessary for these superalloy components. Protective coating is an effective way for this purpose^[3]. The successfully used coatings are mainly two kinds, Al diffusion coatings modified with Cr, Si, Ti, Pt or Hf and overlay MCrAlY coatings (M denotes Fe, Co, Ni or a mixture thereof).

The overlay MCrAlY coatings exhibit good oxidation and hot corrosion resistant performances over a wide temperature range in practical applications. This can be attributed to the stable, dense and adherent Al_2O_3 films covering the entire surface of these coatings and the diffusion of aluminum from the coating to the surfaces to rehabilitate protective films in case of the occurrence of crack and spallation due to thermal cycling. The active elements addition, such as yttrium, tantalum, zirconium, hafnium and silicon to the coatings may surely improve their oxidation resistance and the enhance adherence of the Al_2O_3 film $^{[4\sim7]}$. MCrAlY coatings are typically utilized in the first stages of the turbine where the highest temperature and harshest environment is encountered.

M CrAlY coatings can be prepared by several techniques including the electron beam physical vapor deposition (EBPVD), plasma spraying (mainly low pressure plasma spraying, LPPS), cladding, and arc

plasma deposition (APD) [8~10]. In the LPPS process, the inert and low pressure environment maximizes coatings cleanliness, adhesion and density. It is also easy to change the composition of coating to serve the above purpose. Today LPPS process has become an advanced technique for preparing high performance coatings.

2 EXPERIMENTAL

2. 1 Material and deposition

The NrCorCrAFY-Ta coatings were produced in a DYDP-1 type LPPS unit equipped with a computerized robot with six axes. The chemical composition of the powder used is 20% Cr-23% Co-8.5% Al-0.6% Y-4% Ta and the balance nickel. Its particle size was – 38 \mum. The turbine blades are made of a directionally solidified nickel base superalloy. The coating thickness was 50~80 \mum, samples of 5 mm thick flat plates from the same source as blade were utilized for microstructural observation. Bonding strength tests were performed using a cylindrical test specimen 25.4 mm in diameter. The thickness of the coating tested was about 0.2 mm or so.

The substrates were grit blasted with $120^{\#}$ white alumina. Its average diameter was $125 \, \mu m$.

A constant substrate temperature during deposition is very important, affecting the coatings deposition efficiency, microstructure, and especially the adhesive strength. The substrate temperature is influenced by substrate preheating, vacuum chamber pressure, distance between gun and substrate, plasma gas composition, plasma energy and substrate characteristics such as dimensions and thermal conductivity. In this study, the substrates were cleaned and preheated

at 700~ 800 °C. Reverse transferred arc treating is an efficient method to preheat the substrate. Specimens without reverse transferred arc treating were also coated for comparison.

2. 2 Heat treatment

After deposition, the as-sprayed coatings were heat treated at 1 080 °C for 4 h followed by 870 °C for 32 h in vacuum ($p = 10^{-2} \sim 10^{-3}$ Pa). The cooling rates were: from 1 080 °C to 870 °C in 30 min and from 870 °C to less than 100 °C in 10 h.

2. 3 Evaluation of coating

The microstructures of the coatings were examined by optical microscopy (OM). Electron microprobe analysis (EMPA) was used to determine the composition of the heat treatment samples. The bonding strength between coating and substrate was measured according to ASTM C-633 standard and the hardness of the coating was tested with a Vickers hardness tester using a load of 2 N.

Cyclic hot corrosion tests were carried out at 900 ±10 °C in the combustion medium with 0.005% sea salt solution, consisting of a 55 min exposure to the burner combustion products followed by 5 min of cooling with compressed air at ambient temperature, 150 cycles were tested. Surface morphologies and microstructure changes of the coatings during and after cyclic oxidation were observed.

3 RESULTS AND DISCUSSION

3. 1 Optimization of process parameters

The process parameters, including vacuum chamber pressure, spraying distance, type of nozzle, flow of the plasma gas, plasma energy, powder feed rate, etc, have to be optimized, so that the amount of unmelted powder particles and porosity of the coatings can be controlled to satisfactory level. In this study, various operational modes were examined, and the metallographic structure of the resulting coating including the amount of unmelted particle microcracks, porosity, amounts of oxides or secondary phases at the coating/substrate interfaces, etc, were analyzed. Based on the results, the optimal coating parameters may be obtained.

The powder characteristics, namely, particle size, size distribution, shape and its surface state, have significant effect on the coating quality. For example, the energy levels of the spraying plasma are based on the size distribution. A high energy will result in the gasification of the fine particles, and thus the contamination of the coatings, on the contrary, a low energy will increase the amount of unmelted particles and porosity in the coating. Therefore the powder suitable for high-quality coatings must require a narrow particle distribution. The particle distribution

of the powder used in this study is presented in Fig. 1, showing a rather even distribution with approximately 20% of the fine particles (less than $10\,\mu m$). This distribution requires a more strict control over the plasma energy.

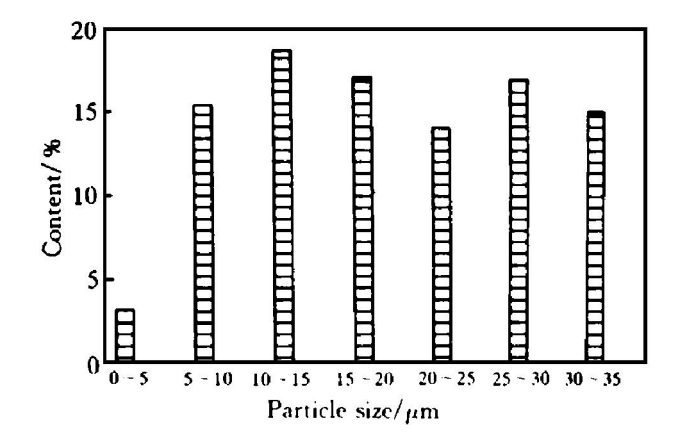


Fig. 1 Particle size distribution of spray powder content

All other processing parameters were held constant, six levels of plasma energy, i. e., 32, 34, 36, 38, 42 and 45 kW, have been used to prepare the coatings and the resulting coatings have been analyzed. Results show that at high energy (42 kW and 45 kW), dense coating can be obtained, however, there are black ash-like inclusions in the coating resulting from the gasified fine particle (Fig. 2(c)) and at low energy (32 kW and 34 kW), more inclusions are found due to unmelted particles (Fig. 2(a)). Fig. 2(b) shows that a dense coating with less unmelted particles can be obtained with proper plasma energy. Optimal coating parameters giving uniform and dense coatings are listed in Table 1.

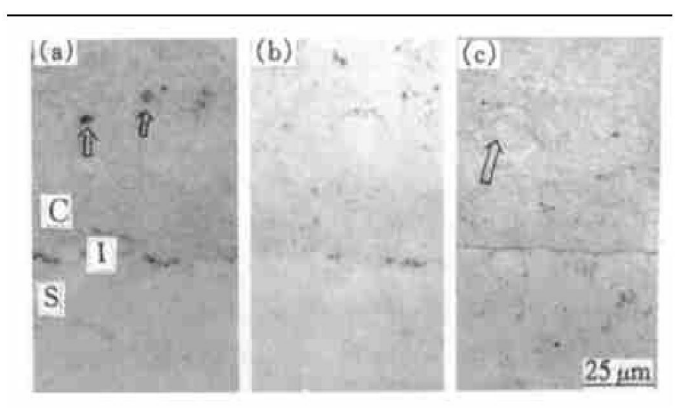


Fig. 2 Effects of plasma energy on coating structure (C= coating, I= interface, S= substrate)

- (a) -34 kW, coating contents with unmelted powder particles (indicated by arrows);
- (b) -38 kW, coating with dense and homogeneous structure;(c) -45 kW, coating with a lamellar structure (indicated by arrow)

The powder used in this experiment is prealloyed. Fig. 3 shows the SEM morphology of the powder. It shows that the shape of powder is spherical with few surface defects. This ensures constant

Table 1 LPPS NiCoCrAlYTa parameters

Parameter	Level
Chamber pressure/kPa	11~ 15
Plasma gas Ar/ (L•min ⁻¹)	40~ 50
$H_2/(L^{\bullet}min^{-1})$	2~ 5
Gun current/ A	500~ 550
Gun voltage/ V	70~ 72
Powder feed/(g•min ⁻¹)	25~ 30
Carrier gas Ar/(L•min ⁻¹)	3~ 5
Spraying distance/mm	280~ 350

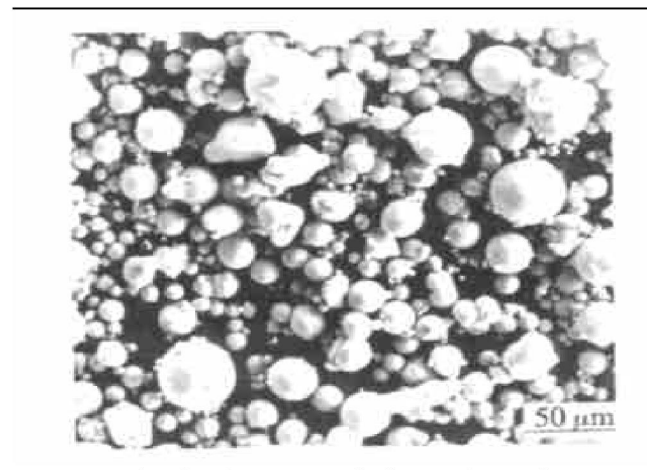


Fig. 3 SEM morphology of powder

powder feed rate and thus a strict control of the coatings thickness.

3. 2 Effect of reverse transferred arc treatment and control of its parameters

As we know, the surface condition has important effect on the adhesive strength between coatings and substrate. The transferred arc is of great significance for substrate pretreatment of the LPPS coating. Under the reverse transferred arc treatment whose work-pieces are taken as negative electrodes, the contaminants and oxidation products on their surfaces can be removed by sputtering. The work-pieces are heated to the desired temperature at the same time. Thus hot and clean work-piece surfaces are obtained, leading to higher adhesive strength. The adhesive strength shows a 40% increase after the reverse transferred arc treatment, measured by tensile tests according to ASTM C-633, as shown in Table 2.

Table 2 Comparison of coating bond strength results

Surface	Coating	Adhesive strength/ MPa			
pretreatment	thickness/µm	1	2	3	Average
Sand blast	200~ 230	42	41	50	44
+ transferred arc	210~ 230	58	65	62	61.7

For smaller and shaped turbine blades, the cleaning and preheating with the reverse transferred arc should be under careful control, so as to obtain a clean surface at expected preheating temperature

without any overheating the blade tips. Increases of the transferred arc current and plasma energy are advantageous to the cleaning, but the overheating of the blade tips should be avoided. To change the movement of spraying gun is also effective for improving the cleaning and shortening the time for cleaning and preheating.

Coatings without thorough cleaning will result in poor adhesive strength due to the oxidation products and contaminants on the coatings/substrate interfaces. The coatings will also undergo delamination from the substrate without sufficient preheating, as shown in Fig. 4.

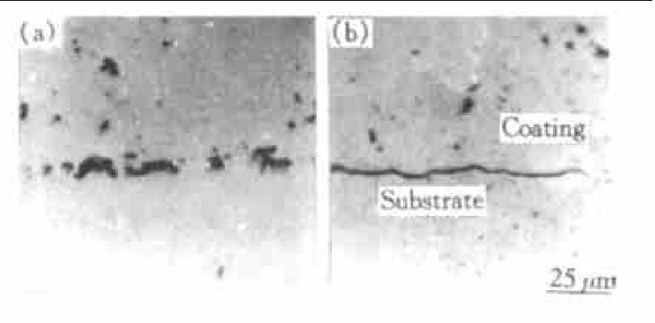


Fig. 4 Illustration of poor coating adherence
(a) —Substrate without thorough cleaning resulting in a number of contamination on interface;

(b) —Substrate without sufficient preheating leading to coating spallation

3. 3 Effect of trajectory of robot on coating thickness distribution

The use of robot ensures precise control of part and torch movement and very efficient plasma spraying. Programming is usually done on-line, and the methods as point-to-point lead-through can be used^[11]. With point-to-point lead-through, an operator leads the machine through the path and records specific points that outline the trajectory he wants the robot to follow. He tells the controller what the speed and distance relative to the substrate are.

A point-to-point lead-through method was used to make the preheating and spraying program according to the turbine blade surface configuration. Suitable processing procedures can be developed based on the information of the coating structure and thickness distribution obtained by SEM observations of the blades. The coating thickness values at designated locations are presented in Fig. 5, showing a uniform distribution meeting the device requirements.

3. 4 Metallography of coatings

Figs. 6(a) and (b) show the microstructure of the baseline coating. They indicate that the coating was dense with few unmelted particle. The coating/substrate interface exhibited good adhesive. A thin interdiffusion layer about 10 µm thick formed after heat treatment at coating/substrate interface, indicating a metallurgical bond. Fig. 7 shows the chemical

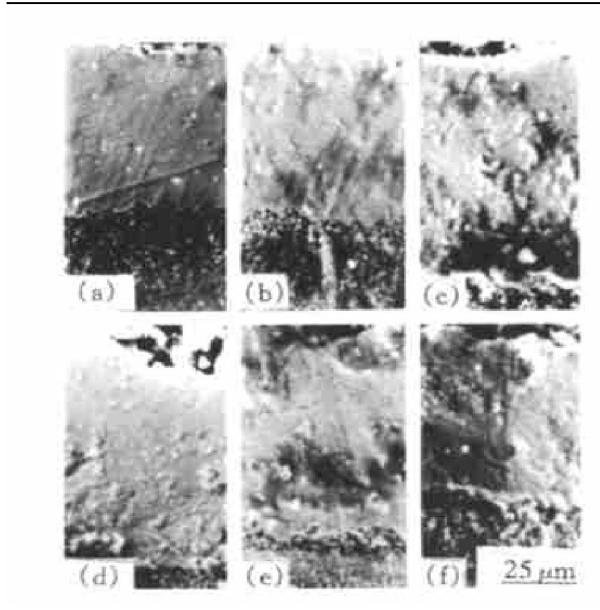


Fig. 5 Coating thickness distribution at pointed area on turbine blade (SEM)

- (a) —Leading edge; (b) —Convex; (c) —Curve;
- (d) Trailing edge; (e) Concave; (f) Terrace

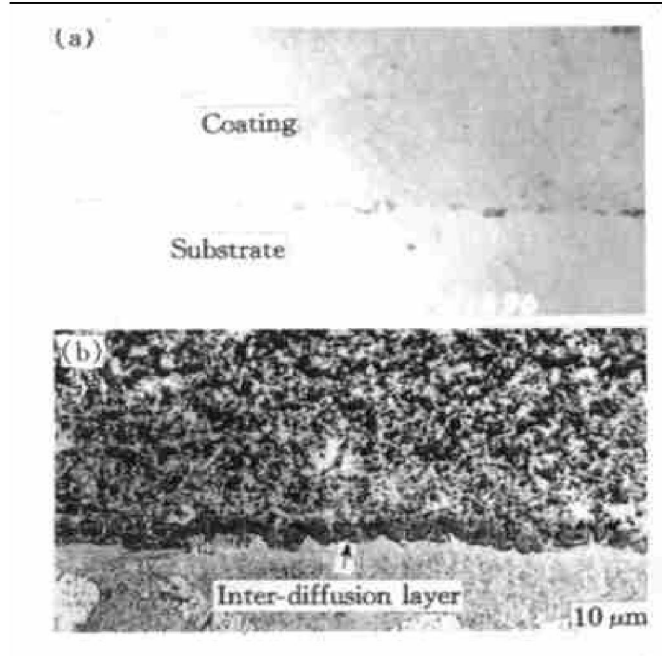


Fig. 6 Optical micrograph of coatings
(a) —As sprayed coating (polished);

(b) —Heat-treated coating (etched)

composition changes at the interface.

3. 5 Phase structure of coatings

Fig. 8 shows the X-ray diffraction patterns of as sprayed coating and heat-treated coating. Y (solid solution of nickel, ordered fcc structure) and β -NiAl phases (bcc structure) are identified both in as sprayed coating and heat-treated coating, while the additional \forall -Ni₃Al phase (fcc structure) has been found in the heat-treated coating.

3. 6 Coating hardness

The Vicker's hardness (10ad, 2N) of the as-

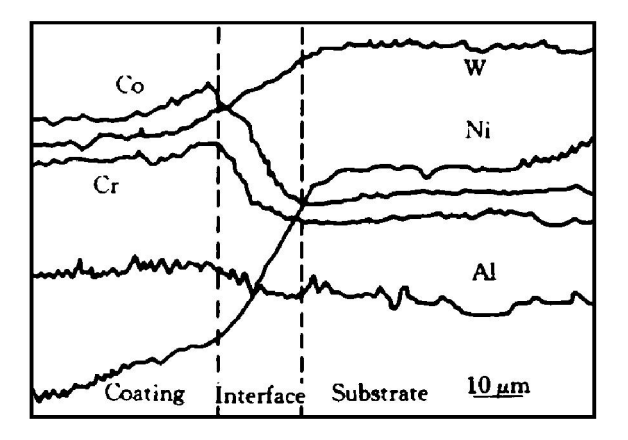


Fig. 7 EPMA line scan across coating/substrate interface of heat treatment sample

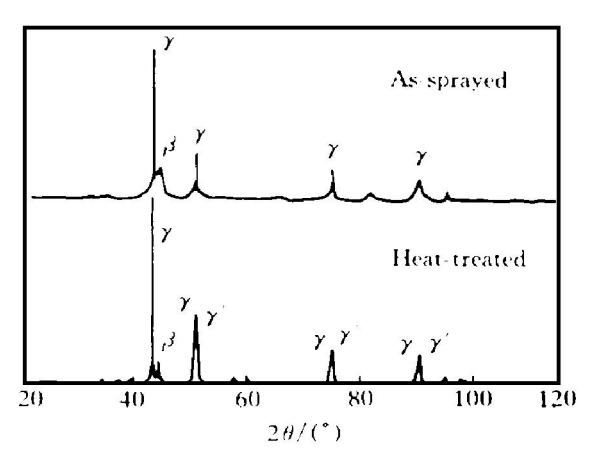


Fig. 8 XRD patterns of coatings

sprayed coating in cross-section is approximately 580 HV. After heat treatment, the hardness value decreases to a level of 450 HV (Table 4). This decrease may be caused by the increased grain size of the heat-treated coatings according to the boundary strengthening mechanism^[9], which can be described by Hallpetch relation $H = H_0 + kd^{-1/2}$ (where H is the hardness, H_0 the intrinsic hardness for a single crystal, k a material constant and d the grain size of the material). The hardness decrease may also be attributed to the disappearance of no equilibrium and supersaturated structures.

Table 4 Micro-hardness results (HV_{0.2})

Sample	1	2	3	4	5	Average
As sprayed	550	570	589	618	580	582
Heat-treated	440	430	460	480	450	452

The hardness values of all the as sprayed samples had a standard deviation of about ±40 HV, while, the heat-treated samples all of about ±20 HV, owing to a more homogeneous composition and microstructure.

3. 7 Cyclic oxidation tests

Cyclic oxidation testing at 900 °C was conducted for two coating systems, namely, sample A1 and A2,

NiCoCrAlYTa (produced in this experiment), sample Bl and B2, aluminized coatings modified with Cr (produced in No. 1 Factory). As it is expected, the LPPS coatings exhibit excellent hot corrosion resistance without spallation and crack, in contrast with the considerable surface deterioration of aluminized samples. The mass loss in an additional alkaline cleaning after 150 cycles oxidation tests also show significant difference, as seen in Fig. 9. The metallographs of the coatings after the oxidation tests are shown in Fig. 10.

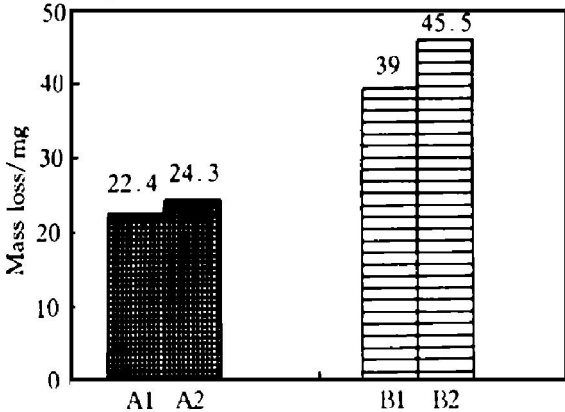


Fig. 9 Mass loss for various coatings after 150 cycles test and additional alkaline cleaning (Cycle consists of 55 min at (900 ±10) ℃ and 5 min of forced air cooling to room temperature)

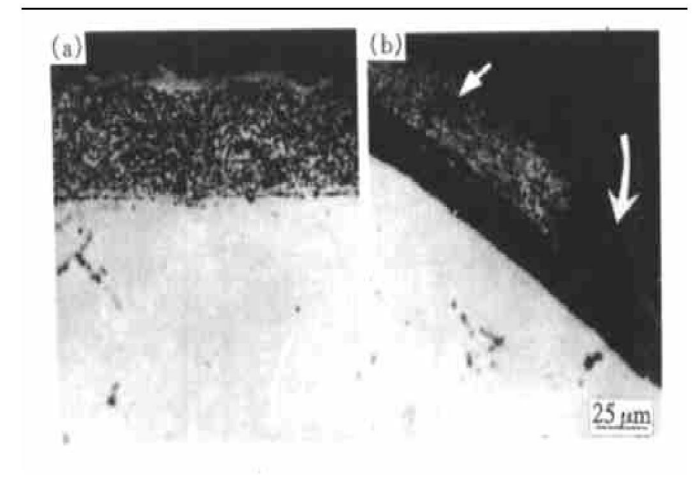


Fig. 10 Coatings morphologies after cyclic oxidation

(a) —Slight surface degradation on LPPS coating;
b) —Considerable surface degradation on aluminized coating,
cracks and partial spallation indicated by arrows

4 CONCLUSIONS

- 1) Transferred arc cleaning method can preheat as well as activate the substrate and lead to the formation of metallurgical bond that enhances adherence of the coating to the substrate.
- 2) The use of synchronized movements between the torch and the blade allows its extremely complex surface to be coated to the required coating thickness distribution.
 - 3) Low pressure plasma spray is a suitable

method for obtaining Nr Cor Cr-Al-Y-Ta coating with low porosity and homogeneous composition. The coating/substrate interface exhibits superior cleanliness. A diffusion zone can also be seen at coating/substrate interface in the heat-treated condition.

4) The cyclic oxidation tests prove that the LPPS coating exhibits superior hot corrosion performance, in contrast with considerable surface spallation of the aluminized coatings.

[REFERENCES]

- Sahoo P, Lewis T F. MCrAlY+ X coatings applied using the high velocity Gator Gard plasma system [A]. Berndt C. Thermal Spray: International Advances in Coatings Technology [C]. Florida, USA. 1992. 75-80.
- [2] JIANG Werr hui, YAO Xiang dong, GUAN Heng rong, et al. Microstructures and properties of DZ40M Corbased superalloy after long-term ageing at 850 °C [J]. Trans Nonferrous Met Soc China, 1998, 8(4): 617-621.
- [3] Liu P S, Liang K M. A new way to evaluate the hightemperature oxidation life of aluminide coatings on Cobased superalloys in air [J]. Surface and Coatings Technology, 2000, 126: 64-68.
- [4] Gudmundsson B, Jacobson B E. The effect of silicon and zirconium additions on the microstructure of vacuum-plasmæsprayed Co-Ni-Cr-Al-Y coatings [J]. Mater Sci Eng, 1989, A108: 73–80.
- [5] Hebsur M G and Miner R V. High temperature tensile and behavior of LPPS NiCoCrAlY coating alloy [J]. Mater Sci Eng, 1986, 83: 239-245.
- [6] Taylor T A, Knapp J K. Dispersion strengthened modified MCrAlY coatings produced by reactive deposition [J]. Surface and Coatings Technology, 1995, 76/77: 34 40.
- [7] ZHENG Tiarr cheng, LUO Yr chun, LI D Y. Erosion behavior of aluminide coating modified with Y addition under different erosion conditions [J]. Surface and Coatings Technology, 2000, 126: 102-109.
- [8] Pekshev P Y, Tcherniakov S V, Arzhakin N A, et al. Plasmæsprayed multiplayer protective coatings for gas turbine units [J]. Surface and Coatings Technology, 1994, 64: 5-9.
- [9] Vetter J, Knotek O, Brand J, et al. MCrAlY coatings deposited by cathodic vacuum arc evaporation [J]. Surface and Coatings Technology, 1994, 68/69: 27–31.
- [10] Boudot A, Monceau D, Pieraggi B, et al. Thermormer chanical characterizations of plasma sprayed MCrAlY coatings for HP turbines [A]. Christian Coddet, Proceedings of 15th International Thermal Spray Conference [C], Nice, France, 1998. 993-998.
- [11] Nylen P, Fransson I, Wretland A, et al. Coating thickness prediction and robot trajectory generation of thermal sprayed coatings [A]. Berndt C. Thermal Spray: Practical Solutions for Engineering Problems [C]. Ohior USA, 1996. 693-697.

(Edited by HE Xue-feng)